

Anomaly in a high-numerical-aperture diffractive focusing lens

Ram Oron, Jacob L. Guedalia, Nir Davidson, and Asher A. Friesem

Department of Physics of Complex Systems, Weizmann Institute of Science, Rehovot 76100, Israel

Erez Hasman

Optical Engineering Group, Faculty of Mechanical Engineering, Technion—Israel Institute of Technology, Haifa 32000, Israel

Received January 3, 2000

We show an anomalous behavior in a diffractive lens in which the spot size at the focus reaches a minimum at a numerical aperture of ~ 0.5 and then increases significantly at higher values. Theoretical and experimental results are presented, along with a comparison with refractive aplanatic lenses, in which the anomaly does not appear to exist. © 2000 Optical Society of America

OCIS codes: 050.1970, 050.1380, 050.1960.

A focusing lens with a high numerical aperture (NA) can focus light into small spots, leading to high resolution and concentration of light. In general, focusing lenses with low rather than high NA's can be analyzed by use of standard scalar theory, for which paraxial approximations are valid.¹ However, to evaluate the performance of a lens with a high NA one must exploit a more exact formulation that takes into account polarization effects and the nonuniformity of the amplitude over the wave front emerging from the lens, i.e., the apodization factor. A mathematically tractable representation for dealing with polarization was developed by Debye,² and a representation for handling apodization was addressed by Hopkins.³ Later these developments were generalized by Wolf⁴ to analysis of aplanatic refractive lenses (free of spherical aberrations) and then exploited in investigations of the focal distributions of a variety of focusing systems.^{5–9} In all these investigations it was determined that the spot size in the focal plane decreased monotonically.

Here we consider diffractive rather than refractive lenses with high NA's. Fabrication of such lenses recently became possible as a result of advances in computer-generated holograms and photolithographic technology. Diffractive lenses can be formed on single, thin, flat elements and can be designed to be free of aberrations.^{10–12} These advantages can be useful in various applications, including high-density optical storage, high-resolution optical microscopy, and high-resolution photolithography.

In the following we investigate the intensity distribution at and near the focus of a high-NA diffractive lens. First we present a brief review of the theory and then describe the experimental procedure and results. Surprisingly, we illustrate that diffractive lenses with high NA's behave differently than aplanatic lenses. Specifically, unlike the monotonic reduction in spot size with increasing NA that occurs with aplanatic lenses, in diffractive lenses there is an optimum NA value beyond which focusing degrades.

We begin by adapting Wolf's vectorial formulation for a refractive aplanatic lens and show how it can be applied to a diffractive lens. Specifically, we start

with the generalized Debye integral for the field at the focus of a refractive aplanatic lens⁵:

$$\hat{U}(P) = \frac{-i}{\lambda} \iint_{\Omega} A_{\omega} \hat{a}(s_x, s_y) \times \exp[ik(s_x x + s_y y + s_z z)] \frac{ds_x ds_y}{s_z}, \quad (1)$$

where (s_x, s_y, s_z) are the normalized propagation-vector components (direction cosines), λ is the wavelength of illumination, $k = 2\pi/\lambda$, A_{ω} is the apodization factor, and $\hat{a}(s_x, s_y)$ for an \hat{x} -polarized incident wave is given by

$$\hat{a}(s_x, s_y) = \left[\left(1 - \frac{s_x^2}{1 + s_z}\right) \hat{x}; \frac{s_x s_y}{1 + s_z} \hat{y}; -s_x \hat{z} \right]. \quad (2)$$

The apodization factor A_{ω} is based on conservation of energy and geometrical factors. For the aplanatic lens it is⁵ $A_{\omega} = \cos^{1/2} \theta$, whereas for a diffractive lens we found it to be $A_{\omega} = 1/\cos^{3/2} \theta$, where θ is the focusing angle (zero at the center of the lens and maximal at the edge of the lens). These apodization factors indicate that the rays at the edge of a diffractive lens have a larger amplitude than those in the center, whereas those in the center have a larger amplitude than at the edge in an aplanatic lens.

Using Eq. (1), we calculated the intensity distribution at the focal plane as a function of NA, from which we deduced the spot size. For these calculations we used two criteria. One was based on the first zero and the other on the encircled 84% of the energy (which corresponds to the first lobe of the Airy pattern). The results are presented in Fig. 1. As shown in the figure, for a low NA, for which the scalar theory is valid, the spot size is the same for both aplanatic and diffractive lenses, regardless of which criterion is used, so the spot size obeys $r = 0.6\lambda/\text{NA}$. As the NA increases, the spot size of the aplanatic lens,

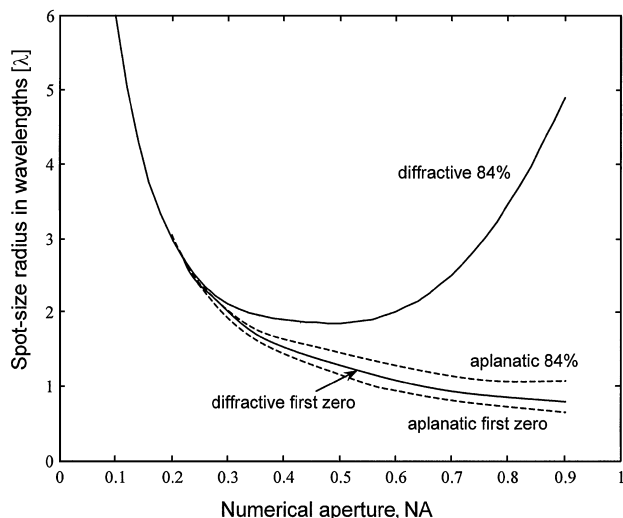


Fig. 1. Calculated spot size as a function of NA for diffractive (solid curves) and aplanatic (dashed curves) lenses. The spot sizes are based on first-zero and 84% encircled-energy criteria.

based on the two criteria, as well as the spot size of the diffractive lens, based on the first-zero criterion only, decrease monotonically, which can still be reasonably expected from the scalar theory. However, when we use the 84% encircled-energy criterion for the diffractive lens, the results reveal that there is a minimum spot size near $NA \approx 0.5$, beyond which the spot size increases significantly. These results indicate that the aplanatic lens concentrates energy better than the diffractive focusing lens when $NA > 0.4$. We found that the same behavior would occur had we chosen other percentages of encircled energy.

The spreading out of the energy for the diffractive lens at a high NA can be attributed to polarization and apodization effects. The polarization of the majority of the encircled energy at the focus is either in the same direction as that of the polarization of the incident wave \hat{e}_x or in the direction of the optical axis \hat{e}_z . Now, the field with polarization direction \hat{e}_x is proportional to J_0 , which is well localized about the origin, and that with \hat{e}_z is proportional to J_1 , which is not localized.¹³ As the NA increases, the encircled energy with the polarization in direction \hat{e}_z increases, whereas that with direction \hat{e}_x decreases. Thus, as the encircled energy with polarization in direction \hat{e}_z becomes dominant, there is more spreading. The other effect that contributes to the spreading of the encircled energy for the diffractive lens results from the apodization factor. Specifically, the amplitudes of the rays at the edge of the lens are larger than those at the center, so the lens behaves as one having an effective annular aperture that transfers energy from the main lobe to the sidelobes. Similar trends were observed in the calculations of Schmitz and Bryngdahl.¹⁴

To verify our surprising predictions we resorted to using a cylindrical rather than a spherical diffractive lens because it was easier to fabricate and evaluate. Specifically, we designed a cylindrical diffractive

lens with a spherical grating function that would be used with $\lambda = 10.6 \mu\text{m}$ from a CO_2 laser and would have a focal length of $f = 10 \text{ mm}$ and an aperture of 30 mm to obtain a NA of 0.83. The lens was fabricated as a binary surface grating in a ZnSe substrate by use of an electron-beam-generated mask, photolithographic technology, and an accurate reactive ion etching process.

For the experiments we illuminated the lens with a collimated Gaussian wave having a sufficiently large waist size that it behaved nearly as a plane wave. The NA was varied by means of a variable aperture. We then measured the energy distributions at and near the focal plane with a knife-edge, with the narrowest distribution at the focal plane. The knife-edge position was controlled by accurate translation stages with resolution better than $0.05 \mu\text{m}$. For the energy measurements we used a pyroelectric detector with a large acceptance angle, which was positioned behind the knife-edge. Accurate alignment was obtained with a coaligned He-Ne laser beam.

Great care was taken during the experiments. For example, to ensure that the incident beam was of high quality, we let it propagate several meters in free space and then measured the beam quality, both with a focusing lens having a focal length of 1 m and with an M^2 meter. Both measurements resulted in an M^2 value of ~ 1.3 . Also, we measured the diffraction efficiency of the lens at various locations and found it to be $40 \pm 10\%$, which agrees with the binary grating prediction. To obtain the intensity distribution we calculated the derivative of the measured energy behind the knife-edge. To reduce noise we averaged a few measurements of the energy.

Figure 2 shows the measured energy at the focal plane as a function of the knife-edge position for three different NA values that correspond to apertures of 6, 16, and 25 mm. The incident beam was TE polarized. As is evident from the figure, the maximal slope is steeper for the higher NA values, as predicted.

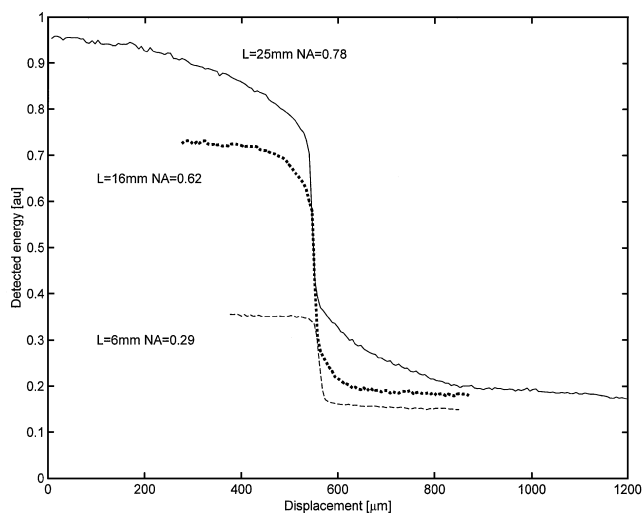


Fig. 2. Detected energy at the focal plane as a function of knife-edge displacement for different NA's and corresponding apertures L .

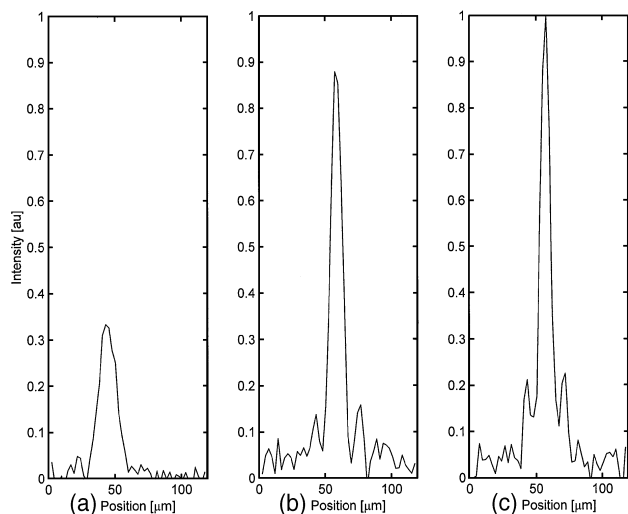


Fig. 3. Intensity distributions at the focus for (a) NA = 0.29, (b) NA = 0.62, (c) NA = 0.78.

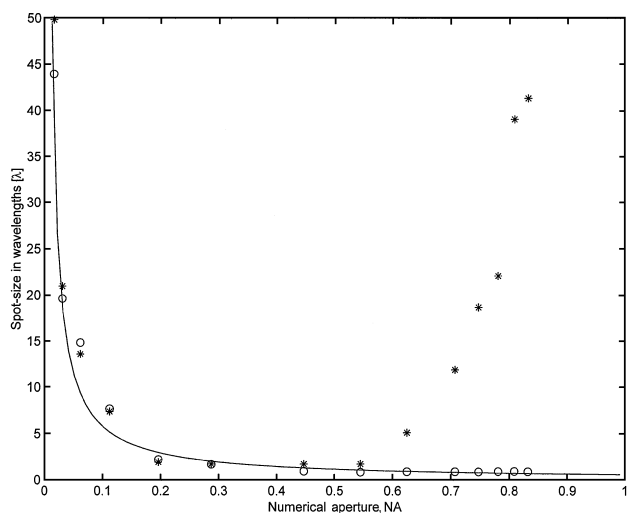


Fig. 4. Experimental spot size as a function of NA for a diffractive cylindrical lens. Asterisks, 72.5% encircled-energy criterion; circles, FWHM criterion; solid curve, the scalar approximation.

However, a larger portion of the energy spreads out away from the focus. Figure 3 shows the three corresponding energy distributions (which are the derivatives of the detected energies in Fig. 2). As is evident from Fig. 3, the main lobe is narrower for higher NA values, which agrees with the predicted first-zero criterion. However, the sidelobes for the higher NA values are high and contain a significant portion of the total energy, indicating spreading of the energy. Fig-

ure 4 shows the spot size as a function of NA for the FWHM and the 72.5% encircled-energy criteria; for the cylindrical lens, 72.5% of the encircled energy corresponds to the FWHM for the one-dimensional scalar case (sinc^2 function). As is evident from the figure, the FWHM decreases monotonically for all NA values, in agreement with prediction and the scalar theory, which is shown in Fig. 4 by a solid curve for $M^2 = 1.3$. For high NA values the spot sizes (when the FWHM criterion is used) reach approximately 0.7λ ($8\ \mu\text{m}$). However, the spot size when the criterion of 72.5% of the encircled energy is used first decreases for low NA values, then reaches a distinct minimum of 1.7λ at approximately $\text{NA} \approx 0.5$, and finally increases very rapidly until it reaches a value of approximately 40λ at $\text{NA} = 0.83$ (30-mm aperture). Similar measurements for σ (energy-distribution standard deviation) showed similar trends, albeit with somewhat less-sharp effects owing to background noise that arises mainly from the zero-order diffraction. Measurements with a TM-polarized beam showed similar trends.

To summarize, we have shown an anomaly in which the energy spreads outward at the focus of a diffractive lens when the NA increases, thereby degrading the effective spot size. This behavior goes against intuition and common wisdom. We believe that one could minimize this spread of energy by forming the diffractive lens on a curved surface or resorting to the use of a hybrid diffractive–refractive lens.

This research was supported in part by the Israeli Ministry of Science. The authors thank Einat Peled for her help with the experimental setup. R. Oron's e-mail address is feoron@weizmann.weizmann.ac.il.

References

1. J. W. Goodman, *Introduction to Fourier Optics* (McGraw-Hill, New York, 1968), p. 64.
2. P. Debye, *Ann. Physik* **30**, 755 (1909).
3. H. H. Hopkins, *Proc. Phys. Soc. London* **55**, 116 (1943).
4. E. Wolf, *Proc. R. Soc. London Ser. A* **253**, 349 (1959).
5. B. Richards and E. Wolf, *Proc. R. Soc. London Ser. A* **253**, 358 (1959).
6. C. J. R. Sheppard, A. Choudhury, and J. Gannaway, *Microwaves Opt. Acoust.* **1**, 129 (1977).
7. A. Yoshida and T. Askura, *Optik* **40**, 322 (1974).
8. R. Barakat, *Appl. Opt.* **26**, 3790 (1987).
9. C. J. R. Sheppard and T. Wilson, *Proc. R. Soc. London Ser. A* **379**, 145 (1982).
10. J. Kedmi and A. A. Friesem, *J. Opt. Soc. Am. A* **3**, 2011 (1986).
11. Y. Amitai and A. A. Friesem, *Opt. Lett.* **13**, 833 (1988).
12. E. Hasman, N. Davidson, Y. Danziger, and A. A. Friesem, *Fiber Integr. Opt.* **16**, 1 (1997).
13. A. Carswell, *Phys. Rev. Lett.* **15**, 647 (1965).
14. M. Schmitz and O. Bryngdahl, *Opt. Commun.* **153**, 118 (1998).